

# **“On direction finding of an emitting source from time delays”**

Author 1: Baruch Berdugo

The Julius Silver Institute of Biomedical Engineering

Technion - IIT ; Haifa 32000 Israel

Author 2: Miriam A. Doron

RAFAEL. Dep. 23, Haifa 31021, ISRAEL

Author 3: Judith Rosenhouse

The Department of General Studies

Technion - IIT ; Haifa 32000 Israel

Author 4: Haim Azhari

The Julius Silver Institute of Biomedical Engineering

Technion - IIT ; Haifa 32000 Israel

Running title: On direction finding

Received:

Correspondence: Dr. Haim Azhari  
Department of Biomedical Engineering  
Technion - IIT  
Haifa 32000 Israel  
Tel: 972 4 829 4130; Fax: 972 4 823 4131  
E-Mail [Haim@Biomed.Technion.ac.il](mailto:Haim@Biomed.Technion.ac.il)

## **Abstract**

This paper presents a statistically and computationally efficient algorithm for direction finding of a single far field source using a multi-sensor array. The algorithm extracts the azimuth and elevation angles directly from the estimated time delays between the array elements. Hence, it is referred to herein as the Time Delay Direction Finding (TDDF) algorithm. An asymptotic performance analysis, using a small error assumption, is conducted. For any 1-D and 2-D array configurations, it is shown that the TDDF algorithm achieves the Cramer Rao Lower Bound (CRLB) for the azimuth and elevation estimates provided that the noise is Gaussian and spatially uncorrected and that the time delay estimator achieves the CRLB as well. Moreover, with the suggested algorithm no constraints on the array geometry are required. For the general 3-D case the algorithm does not achieve the CRLB for a general array. However it is shown that for array geometries which obey certain constraints the CRLB is achieved as well.

The TDDF algorithm offers several advantages over the beamforming approach. First, it is more efficient in terms of computational load. Secondly, the azimuth estimator does not require the a-priory knowledge of the wave propagation velocity. Thirdly, the TDDF algorithm is suitable for applications where the arrival time is the only measured input, in contrast to the beamformer, which is not applicable in this case.

**PACS # 43.60.Gk , 43.60.Cg**

# **1. Introduction**

In various applications of array signal processing such as radar, sonar and seismology, there is a great interest in detection and localization of wideband sources<sup>1</sup>. The problem of estimating the direction of arrival (DOA) of wideband sources using a sensor array has been studied extensively in the literature<sup>2-14</sup>. A common approach<sup>2-7</sup> to this problem, for a single source scenario, is to use the time delay estimation between two sensors to determine the DOA. Many techniques for estimating the travel time delay between *two* receiving sensors have been investigated, see *e.g.*<sup>2-7</sup>. For the *single* source and a *multi-sensor* case, Hahn and Tretter<sup>8</sup> introduced the Maximum Likelihood (ML) delay-vector estimator. ML DOA estimators for the multi sensors and multi sources case have also been studied extensively<sup>12-14</sup>.

It is well known<sup>11</sup> that the ML DOA estimator, for the single source case with a spatially uncorrelated noise, can be realized as a focused beamformer. In this paper an alternative approach is proposed, in which the DOA is extracted directly from the estimated time delays between the array elements (referred to as the time delay vector). This approach is an extension to the multi-sensor case, of the work in<sup>10,11</sup>, where the DOA is extracted from the time delay between *two* sensors for the far field case.

The suggested Time Delay Direction Finding (TDDF) algorithm utilizes the linear relationship between the time delay vector and the DOA vector in Cartesian coordinates. This linear relationship allows a closed form estimation of the DOA vector. The transformation to polar coordinates *i.e.* azimuth and elevation is straightforward for 1-D and 2-D array geometrics. For arbitrarily chosen 3-D array configurations, the best estimator requires a simple non-linear least squares

minimization. Alternatively, a closed form suboptimal solution for the 3-D configuration is also suggested. Finally it is shown that the TDDF azimuth and elevation estimator achieves the CRLB provided that the time delay estimators achieves the CRLB as well

## **2. Methods**

### **2.1 The Time Delay Direction Finding (TDDF) Algorithm:**

Consider an array of  $M$  identical omni-directional sensors with a known arbitrary geometry measuring the wavefield generated by a single farfield wideband source in the presence of an additive noise. Let  $\vec{\mathbf{r}}_i$  denote the location of the  $i$ -th sensor, where  $\vec{\mathbf{r}}_i = [x_i, y_i, z_i]$  for the 3-D array,  $\vec{\mathbf{r}}_i = [x_i, y_i]$  for the 2-D case, and  $\vec{\mathbf{r}}_i = [x_i]$  for the 1-D case, and let  $\mathbf{f}$  and  $\mathbf{q}$  denote the azimuth and elevation angles of the radiating source, respectively (see Fig. 1).

Let us now define the differential delay vector,

$$\vec{\mathbf{t}} = [\tau_{12}, \tau_{13}, \dots, \tau_{1,M}]^T; \quad \mathbf{t}_{1j} \equiv \mathbf{t}_j - \mathbf{t}_1, \quad (1)$$

where the first sensor serves as a reference. The signal DOA vector for the far field case is given by:

$$\vec{\mathbf{k}} = \begin{bmatrix} k_x \\ k_y \\ k_z \end{bmatrix} = \begin{bmatrix} \sin(\mathbf{q}) \cos(\mathbf{f}) \\ \sin(\mathbf{q}) \sin(\mathbf{f}) \\ \cos(\mathbf{q}) \end{bmatrix}. \quad (2)$$

The time delay between any two sensors is equal to the projection of the distance vector between them along the  $\vec{\mathbf{k}}$  vector divided by the sound velocity. Consequently, the delay vector can be expressed as follows:

$$\vec{\mathbf{t}} = -\frac{\mathbf{R}\vec{\mathbf{k}}}{c}; \quad \mathbf{R} \equiv \begin{bmatrix} \vec{r}_2 - \vec{r}_1 \\ \vdots \\ \vec{r}_M - \vec{r}_1 \end{bmatrix} \quad (3)$$

where  $c$  is the wave velocity and the matrix  $\mathbf{R}$  is composed of the distance vectors between all the sensors and the reference sensor.

The objective is to estimate  $\vec{\mathbf{k}}$  from the measured time delay vector  $\vec{\mathbf{t}}$ . Studying Eq.(3), it is evident that the problem is overdetermined. Thus, it is suggested to apply the least squares (LS) method to obtain the estimation. Defining the error as the difference between the measured time difference vector and the evaluated time vector (calculated from the assumed  $\vec{\mathbf{k}}$  vector), the error vector is given by:

$$\vec{\mathbf{e}} = \left( \frac{\mathbf{R}\vec{\mathbf{k}}}{c} + \hat{\mathbf{t}} \right). \quad (4)$$

In the general case, the measurement errors of the time delay vector need not be uncorrelated. Hence, the solution depends on the covariance matrix  $\Lambda_{\mathbf{t}}$  of the delays measurements which is defined by,

$$\Lambda_{\mathbf{t}} = E\{\hat{\mathbf{t}}\hat{\mathbf{t}}^T\} - E\{\hat{\mathbf{t}}\}E\{\hat{\mathbf{t}}\}^T = \text{COV}\{\hat{\mathbf{t}}\}, \quad (5)$$

where  $E\{\}$  denotes the expected value operator. The problem is “over determined” for  $M > 3$ . The LS solution for  $\hat{\vec{\mathbf{k}}}$ , the DOA vector, in this case is given by<sup>15</sup>:

$$\hat{\vec{\mathbf{k}}} = \underset{\vec{\mathbf{k}}}{\text{ArgMin}} \left\{ \left( \frac{\mathbf{R}\vec{\mathbf{k}}}{c} + \hat{\mathbf{t}} \right)^T \Lambda_{\mathbf{t}}^{-1} \left( \frac{\mathbf{R}\vec{\mathbf{k}}}{c} + \hat{\mathbf{t}} \right) \right\} \quad (6)$$

$$= -c(\mathbf{R}^T \Lambda_t^{-1} \mathbf{R})^{-1} \mathbf{R}^T \Lambda_t^{-1} \hat{\mathbf{t}} \equiv -c \mathbf{B} \hat{\mathbf{t}},$$

Thus, estimating the DOA vector becomes a simple multiplication between the measured time delay vector  $\hat{\mathbf{t}}$  and a data independent matrix  $\mathbf{B}$ . The matrix  $\mathbf{B}$  depends on the array geometry (through  $\mathbf{R}$ ) and the time delay covariance matrix which under the assumption of spatially uncorrelated noise is known a-priory up to a multiplicative factor which cancels out in this equation. Consequently, it can be calculated off-line.

In order to express the DOA vector in terms of azimuth and elevation, one has to write the vector  $\hat{\mathbf{k}}$  in a polar coordinate representation. For a 1-D array configuration only  $\hat{k}_x$  can be estimated. Hence, assuming horizontal elevation, the azimuth angle is given by:

$$\hat{\mathbf{f}} = \cos^{-1}(\hat{k}_x). \quad (7)$$

With a 2-D array, both the azimuth and elevation angles can be calculated by:

$$\hat{\mathbf{f}} = \tan^{-1}(\hat{k}_y / \hat{k}_x), \quad (8a)$$

$$\hat{\mathbf{q}} = \cos^{-1}(\hat{k}_z) = \cos^{-1}\left(\left(1 - (\hat{k}_x^2 + \hat{k}_y^2)\right)^{1/2}\right). \quad (8b)$$

For the case of a 3-D array, Eq.(2) yields three non-linear equations with two unknowns  $(\phi, \mathbf{q})$ . Again the problem is over determined. Thus, the azimuth and elevation angles  $(\phi, \mathbf{q})$  can be evaluated as the nonlinear least square estimator solving Eq.(2)

$$(\hat{\mathbf{f}}, \hat{\mathbf{q}}) = \underset{\hat{\mathbf{f}}, \hat{\mathbf{q}}}{\text{ArgMin}} \left\{ \left( \hat{\mathbf{k}} - \bar{\mathbf{k}}(\hat{\mathbf{f}}, \hat{\mathbf{q}}) \right)^T \Lambda_k^{-1} \left( \hat{\mathbf{k}} - \bar{\mathbf{k}}(\hat{\mathbf{f}}, \hat{\mathbf{q}}) \right) \right\}, \quad (9)$$

where  $\Lambda_{\hat{\mathbf{k}}}$  is the covariance matrix of vector  $\hat{\mathbf{k}}$ , which is given in Appendix A (Eq.(14)).

An alternative simplified close-form suboptimal estimate is proposed by:

$$\hat{\mathbf{f}} = \tan^{-1}(\hat{k}_y / \hat{k}_x), \quad (10a)$$

$$\hat{\mathbf{q}} = \tan^{-1}\left(\left(\hat{k}_x^2 + \hat{k}_y^2\right)^{1/2} / \hat{k}_z\right). \quad (10b)$$

In appendix A. the performance of the TDDF algorithm is analyzed, and it is shown that it is asymptotically efficient. Furthermore, it is shown that under certain geometrical constrains for the sensors arrangement even the closed form 3-D solution achieves the CRLB .

Importantly, it should be noted, that the azimuth estimates given above for the 2-D and 3-D array configurations, are independent of the wave velocity  $c$ , (stems from the fact that the solutions are given in terms of the ratio between  $\hat{k}_y$  and  $\hat{k}_x$ , and both are a linear function of  $c$ ). Therefore, errors in the assumed sound speed will not induce errors in the azimuth angle.

## **2.2 Performance analysis**

In appendix A. the covariance matrix for  $(\hat{\mathbf{f}}, \hat{\mathbf{q}})$  is calculated. The performance of the TDDF estimator is compared to the theoretical CRLB. It is shown that for the 1-D and 2-D cases the estimator is asymptotically efficient since it achieves the bound. For the 3-D case the closed form estimator given in Eq.(10) is not always efficient. However, we derived constrains on the array geometry in which the CRLB is also achieved.

## **3. Results**

In this section, the performance of the TDDF algorithm is demonstrated via numerical simulations and by experimental results.

### **3.1 Numerical Simulations**

Simulations were conducted for 2-D and 3-D arrays. The 2-D array was comprised of randomly located 7 sensors, as shown in Fig. 2(a). In the first set of simulations the source was positioned at a fixed location with an azimuth angle of  $60^0$  and an elevation of  $30^0$ . The SNR was scanned in the range of -10dB to +10dB, the integration time was  $50ms$ , and the frequency bandwidth was 500-1500Hz. The noisy estimates of the time delay vectors were generated as Gaussian random vectors with a covariance matrix  $\Lambda_t$  given in equation Eq.(12). The propagation velocity was taken to be 340m/sec.

Five hundred Monte Carlo runs were performed for each SNR value. The azimuth angle was calculated with the TDDF algorithm and the corresponding errors were computed. The standard deviation of the localization errors was then estimated. For comparison, the CRLB was also calculated as explained in appendix A. The results are depicted in Fig.3. For clarity of presentation, only 50 azimuth estimation errors are plotted (as small dots) at each SNR level. The standard deviation of the TDDF estimator are depicted as circles and the corresponding CRLB is depicted as a solid line for the entire range. It can be seen that the standard deviations of the TDDF estimator are effectively located on the CRLB line (in accordance with the mathematical derivation given in appendix A).

In a second set of simulations, the same 2-D array was used. The SNR was held fixed at -6dB. The elevation angle was set to  $50^\circ$ , and the azimuth angle was scanned in the range of  $0^\circ - 360^\circ$ . The corresponding CRLB line was calculated and the standard deviation of the TDDF estimator was evaluated for each angle. Figures 4(a) and 4(b) display the errors of the TDDF algorithm for the azimuth and elevation, respectively. From these curves it is observed that the TDDF estimator achieves the CRLB, both in azimuth and elevation, for a 2-D array with an arbitrary geometry.

In the third set of simulations the 3-D array shown in Fig. 2(b) was used. This array has 6 sensors equally distributed on a circle with a radius of  $0.1m'$  and the seventh sensor is located  $0.1m'$  above the center of the array. The SNR was again held fixed at -6dB. The azimuth was set to  $20^\circ$ , and the elevation angle was scanned in the range  $0^\circ - 180^\circ$ . The following quantities were calculated this time: the CRLB, the standard deviation of the TDDF estimator, and the theoretical standard deviation calculated from Eq.(25). Figures 5(a) and 5(b) plot these quantities as a function of the elevation angle.

The 3-D array used here obeys the condition given in Eq.(27). Consequently, the CRLB is achieved for the azimuth TDDF estimates (Fig.5(a)). For the elevation angle, however, the obtained estimate errors are larger than the CRLB. This observation is consistent with the fact that the array geometry does not comply with condition given in Eq.(29). Nevertheless, the degradation is moderate for this array configuration. This implies that the closed form estimation given by equation set (10) is sufficiently accurate for practical purposes. Finally it can be observed that the estimated errors match the theoretical standard deviations predicted by Eq.(25). It should also be noted that bias was also estimated in all the above simulation and was

found negligible (two orders of magnitude smaller than the variance contribution to the total error).

In practical applications it is usually not easy to obtain the optimal estimate for the time delay vector  $\tau$ . In the last numerical example we demonstrate the performance of the TDDF algorithm when using a suboptimal estimator for the time delay vector as presented in appendix C. The time delay vector was estimated via a cross-correlation between the reference sensor (#1) and the other sensors. The performance of the TDDF algorithm is compared to that of a beamformer. This simulation uses the 2-D array consisting of 3 microphones which is shown in Fig 2c. The source direction was set at an azimuth of  $30^\circ$  and an elevation angle of  $90^\circ$ . The SNR was scanned in the range of -10dB to +10dB. Here, the simulation generates the time record of the sensor data assuming spatially uncorrected noise. Both the signal and the noise were random Gaussian variables with a bandwidth of 100-3000 Hz. In order to perform the beam steering required in the beamformer the data were interpolated by a factor of 10. The standard deviation error of both estimators was estimated by 100 Monte Carlo runs. The standard deviation of the TDDF estimate are depicted by asterisks in figure 6 while the standard deviation of the Beamformer is denoted by circles. As can be seen for most of the studied SNR range the performance of the TDDF is the same as that of the beamformer. However, the threshold point for the TDDF appears at SNR=-3db which is higher than the threshold observed for the beamformer (-6db). This result is not surprising since the TDDF is not an ML estimator as the beamformer. Potentially there are two factors that can cause the performance of the TDDF to collapse. The first is the time delays vector estimation process, and the second is the nonlinear operation for estimating  $\gamma$ . In all the cases we have tested, the time delay estimate was

the first one to diverge. Practically it was observed that the cross-correlation function have generated spurious peaks at low SNR, and this is probably the main cause for the performance diverges at low SNR.

### **3.2 Experimental Results**

A 3-D array consisting of 7 microphones (AudioTechnica MT350B) arranged in the same configuration depicted in Fig2(b), (Radius=0.1m', height=0.1m'), was used. Two experiments were conducted. In the first experiment the array was located in an anechoic chamber (internal dimension of 1.7 x1.7x1.7 m'). In the second experiment the array was placed in an ordinary room. The sound source was a recorded male voice (Richard Burton) reading a 20-second long sentence. The signal was played via a loudspeaker located 1.5 m' from the array. The outputs of the array were recorded using an 8-channel tape recorder (Sony-pc208A). The time delay between the sensors and the central microphone was estimated by filtering the data by a band pass filter 500-1500 Hz, and performing a cross-correlation process. The integration time was 40 ms, yielding about 500 independent measurements to estimate the system performance. After completion of each set of measurements, the array was rotated by  $30^0$  and the procedure was repeated.

The azimuth angles corresponding to each set of measurements was estimated using the TDDF algorithm. The standard deviation of the errors for the TDDF estimates was then evaluated. The results are outlined in Fig. 7 . The data from the anechoic chamber is denoted by 'o' and the data from the regular room is presented by '\*'. As can be observed the average TDDF error for the anechoic chamber experiment was about  $15^0$ . The second experiment was held in the regular room, and the average

error was about  $5^0$ . This degradation is attributed to the room reverberations and the background noise. We have measured the reverberation time in both rooms. In the anechoic chamber the reverberation time was about 10-ms, while in the regular room the reverberation time was about 250-ms. Thus, we believe that the room reverberation was the major cause for the degradation in the accuracy of the direction estimates.

## **4. Discussion**

This paper presents and analyzes the Time Delay Direction Finding (TDDF) algorithm for a single emitting source using a multi-sensor array. The algorithm extracts the azimuth and elevation angles directly from the estimated time delays between the array elements. The algorithm offers computational simplicity as it utilizes the linear relationship between the time delay vector and the DOA vector in Cartesian coordinates. This linear relationship allows a closed form estimation of the DOA vector.

An asymptotic performance analysis of the TDDF algorithm, using a small error assumption is performed. For the 1-D and 2-D array configurations it is shown that the TDDF algorithm achieves the Cramer Rao Lower Bound (CRLB) provided that the time delay vector estimator achieves the CRLB as well. This was proven mathematically in appendix A and was demonstrated by numerical simulations. For a 3-D array configuration a suboptimal closed form estimator is presented (Eq.(10)). Nevertheless, it is shown that when using array geometries that obey certain constraints the closed form solution also achieves the CRLB. If the array obeys the condition given by Eq.(27), then the azimuth estimation is statistically efficient. Furthermore, if

the array also obeys the constraints that are given in Eq.(29), the estimator is efficient for the elevation angle as well.

Numerical and experimental results were given to demonstrate the performance of the TDDF algorithm. The experimental results with a 7 microphone array have shown that in an anechoic chamber the average TDDF azimuth error was about 1.5 degrees, while in a regular room the average error was about 5 degrees. These results indicate that the TDDF can serve as a practical tool for passive localization of a single radiating source.

The proposed TDDF algorithm offers several advantages over the popular beamforming approach<sup>11</sup>. First, the TDDF algorithm is considerably more efficient in terms of computational load. It calculates the azimuth and the elevation angle directly from the estimated time delays, and does not involve a two dimensional search over the array manifold as the beamformer.

Secondly, for the 2-D and 3-D array configurations, the TDDF algorithm does not require the a-priori knowledge of the propagation velocity to estimate the azimuth, see Eq.(8a) and Eq.(10a). respectively. This property of the TDDF is very useful in acoustic applications where uncertainty in the propagation velocity occurs due to wind and temperature variations<sup>17</sup>. This is contrary to the beamformer, which uses the wave propagation velocity as input. In principle the beamforming process could scan the velocity as an additional unknown parameter, however this would substantially increase the computational load as an additional parameter would have to be scanned.

The third advantage of the TDDF method, arises in applications where the signal is a very short transient and the arrival time of the pulse is directly measured by the system hardware. Since only the time delays are available in this case the

beamforming is not applicable. For TDDF algorithm on the other hand this information is sufficient.

Finally, in certain acoustic and geophysical applications, loss of spatial coherence of the signal received at the sensors may occur if the distance between the sensors is large<sup>1, 17</sup>, thus precluding the use of the beamforming approach. In such cases, nevertheless, time delay between sensors can still be estimated via incoherent processing means, such as time of arrival difference, and the TDDF algorithm is still applicable.

The TDDF has one major disadvantage. It is limited to a single source scenario. The beamformer algorithm on the other hand can localize more than one source, provided that the angular separation between the sensors is more than the beam-width.

## **Acknowledgments**

The authors thank the “Lamar Signal Processing Israel” for providing the facilities and for their assistance in performing the experiments. The support of the Irving and Adeele Rosenberg Foundation Inc., (H.A.) is also acknowledged.

## Appendix A

### Performance Analysis of the TDDF Algorithm

In order to evaluate the performance of the TDDF algorithm, analytic expressions for the accuracy of the azimuth and elevation estimations for the 1-D, 2-D and 3-D cases are first derived. These expressions are then compared to the expression of the CRLB as derived by Neilsen.<sup>16</sup> and cited in Appendix B.

For uniformity and simplicity of notations let us define  $\mathbf{g} = \mathbf{f}$  for the 1-D case, and  $\mathbf{g} = (\mathbf{f}, \mathbf{q})^T$  for the 2-D and 3-D cases. Under the assumption of small errors the covariance matrix of  $\mathbf{g}$  can be expressed as:

$$\Lambda_{\mathbf{g}} = \bar{\nabla}_k \gamma \cdot \Lambda_k \cdot \bar{\nabla}_k^T \gamma = \bar{\nabla}_k \gamma \cdot \bar{\nabla}_t k \cdot \Lambda_t \cdot \bar{\nabla}_t^T k \cdot \bar{\nabla}_k^T \gamma \quad (11)$$

where  $\Lambda_x$  is the covariance matrix of the vector  $\mathbf{x}$ , and  $\bar{\nabla}_x y$  is the gradient (Jacobian) of  $\bar{y}$  with respect to  $\bar{x}$ . Again for a small error assumption it can be verified that the DOA estimates are asymptotically unbiased, thus the covariance matrix represents the total error of the estimator.

Clearly, the performance of the TDDF algorithm depends on the covariance matrix of the time delay vector. To demonstrate the performance of the TDDF algorithm we shall assume that the time delay vector estimator achieves the CRLB. An efficient algorithm for estimation of the time delay vector assuming that both the signal and the noise are zero mean uncorrelated Gaussian processes, and the noise is spatially uncorrelated, has been proposed and studied by Hahn and Tretter<sup>8</sup>. Their work presents an estimator for the time delay vector which achieves the CRLB, and does not require the beamformer process, Their scheme is based on estimating  $M(M-1)$  individual time delays via a pre-filtered correlators. The vector  $\tau$  is obtained by a linear combination of the individual time delays. The covariance matrix for the time delay

vector for this estimator, assuming that the SNR is the same for all the sensors, is given by:

$$\Lambda_t = \mathbf{CRLB}_t = \frac{\mathbf{s}_t^2}{2} [\mathbf{I}_{M-1} + \mathbf{1}_{M-1} \mathbf{1}_{M-1}^T] \quad (12)$$

Where:  $\mathbf{I}_M$  is the MxM Identity matrix,  $\bar{\mathbf{1}}_M$  is an M-dimensional vector of ones,

$$\mathbf{s}_t^2 = \left( \sum_{l=1}^{L_{\max}} (\mathbf{w}_0 l)^2 \mathbf{r}(l) \frac{M\mathbf{r}(l)}{1 + M\mathbf{r}(l)} \right)^{-1}, \text{ and } \mathbf{r}(l) \equiv S(l)/N(l) \text{ denotes the SNR at the}$$

frequency  $(\mathbf{w}_0 l)$ .

In the following it shall be assumed that  $\Lambda_t$  is given by Eq.(12) i.e. efficient estimate of  $\bar{\mathbf{t}}$ ,

In appendix B we derive  $\Lambda_t$  for suboptimal time delay estimator via only (M-1) correlators, using one sensor as a reference sensor i.e. an efficient estimate is only obtained for the separate pairwise delays. It is shown that for sufficiently high SNR this estimator also achieves the CRLB.

First, the covariance matrix of the direction vector  $\bar{k}$  is calculated,

From Eq.(6)

$$\bar{\mathbf{V}}_t^T k = c\mathbf{B} \quad (13)$$

and therefore

$$\Lambda_k = E\{\bar{\mathbf{k}}\bar{\mathbf{k}}^T\} = \mathbf{B}\Lambda_t\mathbf{B}^T c^2 \quad (14)$$

Using the definition of  $\mathbf{B}$  in Eq.(6) and applying some algebraic simplifications yields,

$$\Lambda_k = (\mathbf{R}\Lambda_t^{-1}\mathbf{R}^T)^{-1} c^2. \quad (15)$$

Applying the matrix inversion lemma to Eq.(12) it can be written that

$$\Lambda_t^{-1} = \frac{2}{\mathbf{s}_t^2} \left[ \mathbf{I}_{M-1} - \frac{\bar{\mathbf{1}}_{M-1} \bar{\mathbf{1}}_{M-1}^T}{M} \right]. \quad (16)$$

From the definitions of  $\mathbf{R}$  in Eq.(3) it follows that

$$\mathbf{R} = [-\mathbf{1}_{M-1} \quad \mathbf{I}_{M-1}] \mathbf{P} \quad (17)$$

Where  $\mathbf{P}$  is the sensor position matrix defined by:

$$\mathbf{P} = [\bar{\mathbf{x}}, \bar{\mathbf{y}}, \bar{\mathbf{z}}] = \begin{matrix} \hat{\mathbf{e}}^{x_1} & y_1 & z_1 & \hat{\mathbf{u}} \\ \hat{\mathbf{e}} & : & : & \hat{\mathbf{u}} \\ \hat{\mathbf{e}} & : & : & \hat{\mathbf{u}} \\ \hat{\mathbf{e}}^{x_M} & y_M & z_M & \hat{\mathbf{u}} \end{matrix} \quad (18)$$

Substituting Eq.(16) and Eq.(17) into Eq.(15) yields after some algebraic manipulations:

$$\mathbf{L}_k = \begin{matrix} \mathbf{a} \\ \mathbf{c} \\ \mathbf{e} \end{matrix} \mathbf{P}^T \mathbf{P} \cdot \frac{(\mathbf{P}^T \bar{\mathbf{1}}_M)(\mathbf{P}^T \bar{\mathbf{1}}_M)^T \ddot{\mathbf{0}}^{-1}}{M} \div \frac{\sigma_t^2}{2} c^2. \quad (19)$$

Assuming without any loss of generality that the coordinate origin is in the center of gravity i.e.  $\mathbf{P}^T \bar{\mathbf{1}}_M = \bar{\mathbf{0}}$  we finally get the simple expression for the DOA vector covariance matrix,

$$\mathbf{L}_k = (\mathbf{P}^T \mathbf{P})^{-1} \frac{\mathbf{s}_t^2}{2} c^2. \quad (20)$$

In the following, the expressions for the accuracy of the azimuth and elevation TDDF estimations are derived and compared to the CRLB which is cited in appendix B.

### **A.1 A linear (1-D) array configuration**

For the 1-D case  $\boldsymbol{\xi} = \mathbf{f}$ , and  $\bar{\mathbf{k}} = k_x = \cos(\mathbf{f})$ . Thus

$\bar{\nabla}_k \mathbf{g} = -1/\sin(\mathbf{f})$ ; and  $\Lambda_k = \frac{1}{\sum x_i^2} \frac{\mathbf{S}_t^2}{2} c^2$  inserting into Eq.(11) gives

$$\mathbf{S}_f^2 = \frac{1}{\sin^2(\mathbf{f}) \sum x_i^2} \frac{\mathbf{S}_t^2}{2} c^2 \quad (21)$$

The CRLB for the 1-D case is given by:  $CRLB(\mathbf{f}) = 1/J_{ff}$  (see appendix B).

Substituting  $y_i=z_i=0$  in this expressions yields:

$$CRLB(\mathbf{f}) = \frac{1}{\sin^2(\mathbf{f}) \sum x_i^2} \frac{\mathbf{S}_t^2}{2} c^2$$

As can be observed this expression is identical to the right hand side of Eq.(21),

indicating that the TDDF estimate achieves the CRLB in this case.

### **A.2 A planar (2-D) array configuration**

From Eq.(2) and Eq.(8) the Jacobian  $\bar{\nabla}_k \mathbf{g}$  is given by :

$$\bar{\nabla}_k \boldsymbol{\gamma} = \frac{1}{-\sin(\theta)\cos(\theta)} \begin{bmatrix} -\sin(\phi)\cos(\theta) & \cos(\phi)\cos(\theta) \\ -\cos(\phi)\sin(\theta) & -\sin(\phi)\sin(\theta) \end{bmatrix}. \quad (22)$$

Inserting Eq.(22) and Eq.(20) into Eq.(11) yields,

$$\sigma_\phi^2 = \frac{1}{\sin^2(\theta)} \frac{\cos^2(\phi) \sum x_i^2 + 2 \cos(\phi) \sin(\phi) \sum x_i y_i + \sin^2(\phi) \sum y_i^2}{\sum x_i^2 \sum y_i^2 - (\sum x_i y_i)^2} \frac{\sigma_\tau^2}{2} c^2. \quad (23a)$$

and

$$\mathbf{s}_q^2 = \frac{1}{\cos^2(\mathbf{q})} \frac{\sin^2(\mathbf{f}) \sum x_i^2 - 2 \cos(\mathbf{f}) \sin(\mathbf{f}) \sum x_i y_i + \cos^2(\mathbf{f}) \sum y_i^2}{\sum x_i^2 \sum y_i^2 - (\sum x_i y_i)^2} \frac{\mathbf{s}_t^2}{2} c^2. \quad (23b)$$

Applying a lengthy but straightforward evaluating of the expressions for the CRLB Eq.(A1) for both the azimuth and the elevation angles for the 2-D arrays, i.e.  $z_i=0$ ; shows that they are identical to Eq.(23). Thus, it is concluded that the TDDF algorithm is a statistically efficient estimator for 2-D array, which reaches the CRLB. It is important to note that no constraints on the array geometry were applied.

### **A.3 A spatial (3-D) array configuration**

The estimate of  $\boldsymbol{\xi} = (\phi, \mathbf{q})$  for the 3-D array case involves a nonlinear LS minimization Eq.(9). An alternate close form close-form suboptimal estimator was suggested in Eq.(10). Here we calculate the performance of the sub-optimal estimator and derive the conditions on the array geometry that guarantee statistical efficiency (achieves the CRLB).

From Eq.(2) and Eq.(10) the Jacobian  $\bar{\mathbf{V}}_k \mathbf{g}$  is given by :

$$\bar{\mathbf{V}}_k \mathbf{g} = \begin{bmatrix} -\frac{\sin(\mathbf{f})}{\sin(\mathbf{q})} & \frac{\cos(\mathbf{f})}{\sin(\mathbf{q})} & 0 \\ \cos(\mathbf{q}) \cos(\mathbf{f}) & \cos(\mathbf{q}) \sin(\mathbf{f}) & -\sin(\mathbf{q}) \end{bmatrix}. \quad (24)$$

Using Eq.(11) and Eq.(15)

$$\mathbf{s}_f^2 = \frac{\mathbf{s}_t^2 c^2}{2 \sin^2(\mathbf{q})} [\sin(\mathbf{f}) \quad \cos(\mathbf{f}) \quad 0] (\mathbf{P}^T \mathbf{P})^{-1} [\sin(\mathbf{f}) \quad \cos(\mathbf{f}) \quad 0]^T, \quad (25a)$$

and

$$\mathbf{s}_q^2 = \frac{\mathbf{s}_t^2 c^2}{2} \begin{bmatrix} \cos(\mathbf{q})\cos(\mathbf{f}) & \cos(\mathbf{q})\sin(\mathbf{f}) & -\sin(\mathbf{q}) \end{bmatrix} (\mathbf{P}^T \mathbf{P})^{-1} \cdot \begin{bmatrix} \cos(\mathbf{q})\cos(\mathbf{f}) & \cos(\mathbf{q})\sin(\mathbf{f}) & -\sin(\mathbf{q}) \end{bmatrix}^T \quad (25b)$$

In general this estimator is not efficient. However if the array obeys the following geometrical conditions.

$$\begin{aligned} \sum x_i y_i &= \sum x_i z_i = \sum y_i z_i = 0 \\ \sum x_i^2 &= \sum y_i^2 \end{aligned} \quad (27)$$

then the variance of the azimuth angle estimation is given by

$$\mathbf{s}_f^2 = \frac{1}{\sin^2(\mathbf{q})} \frac{1}{\sum x_i^2} \frac{\mathbf{s}_t^2}{2} c^2 \quad (28)$$

Evaluating the CRLB for the azimuth estimate under the same condition yields an identical expression. Thus, under the conditions outlined in Eq.(27), the TDDF algorithm is also an efficient estimator for the azimuth angle. When studying the conditions for uncoupled estimates of azimuth and elevation angles, Nielsen<sup>16</sup> has also reached the same conditions given in Eq.(27), and gave a few examples of 3-D arrays obeying these constraints.

If we further constrain the array geometry and require a fully balanced array configuration, which obeys the following condition,

$$\sum x_i^2 = \sum z_i^2 \quad (29)$$

in addition to the conditions outlined in Eq.(27), it can be shown that for the elevation estimate,

$$\mathbf{s}_q^2 = \frac{1}{\sum x_i^2} \frac{\mathbf{s}_t^2}{2} c^2 = CRLB_q \quad (30)$$

Thus, under the above conditions the TDDF algorithm achieves the CRLB for both the azimuth and the elevation angles, and is therefore an asymptotically efficient estimator.

## Appendix B- CRLB for the azimuth and elevation angles

Nilsen<sup>16</sup> derived analytic expressions for the Cramer Rao Lower Bound for the estimation errors of the azimuth angle  $\mathbf{f}$  and the elevation angle  $\mathbf{q}$ , using 3-D arrays.

$$\begin{aligned} CRLB(\mathbf{q}) &= J_{ff} / (J_{ff}J_{qq} - J_{\mathbf{f}}^2) \\ CRLB(\mathbf{f}) &= J_{qq} / (J_{ff}J_{qq} - J_{\mathbf{f}}^2) \end{aligned} \quad (31)$$

where

$$\begin{aligned} J_{\phi\phi} &= G \sin^2(\theta) \sum_{i=1}^M [x_i \sin(\phi) - y_i \cos(\phi)]^2 \\ J_{\theta\theta} &= G \sum_{i=1}^M [x_i \cos(\phi) \cos(\theta) + y_i \sin(\phi) \cos(\theta) - z_i \sin(\theta)]^2 \\ J_{\phi\theta} &= G \sin(\theta) \sum_{i=1}^M [x_i \sin(\phi) - y_i \cos(\phi)] [x_i \cos(\phi) \cos(\theta) + y_i \sin(\phi) \cos(\theta) - z_i \sin(\theta)] \\ G &= \sum_{l=1}^{L_{\max}} (\mathbf{w}_0 l) \frac{M \mathbf{r}^2(l)}{1 + M \mathbf{r}(l)} \end{aligned}$$

In these expressions the coordinates origin is in the center of gravity of the array, i.e.

$$\sum x_i = \sum y_i = \sum z_i = 0$$

and the coordinate system is given in Fig. 1



## References

- <sup>1</sup> S. Haykin, Editor, "Array Signal Processing," New Jersey: Prentice-Hall.
- <sup>2</sup> G.C. Carter, "Time delay Estimation for Passive Signal Processing," *IEEE Trans. Acoust., Speech, Signal Processing (Special Issue on Time Delay Estimation)*, vol,ASSP-29. Pp 463-470, June 1981.
- <sup>3</sup> A.H. Quazi, "An Overview on Time Delay Estimation in Active and Passive System for Target Localization," *IEEE Trans. Acoust., Speech, Signal Processing (Special Issue on Time Delay Estimation)*, vol,ASSP-29. Pp 527-533, June 1981.
- <sup>4</sup> A.G. Piersol "Time Delay Estimation Using Phase Data," *IEEE Trans. Acoust., Speech, Signal Processing (Special Issue on Time Delay Estimation)*, vol,ASSP-29. Pp 471-477, June 1981
- <sup>5</sup> C.H. Knapp and G.C. Carter, "The generalized correlation method for estimation of time delay," *IEEE Trans. Acoust., Speech, Signal Processing*, vol. ASSP-24, pp. 320-327, Aug. 1976.
- <sup>6</sup> C. Hassab and R.E. Boucher, "Optimum estimation of time-delay by a generalized correlator," *IEEE Trans. Acoust., Speech, Signal Processing*, vol. ASSP-27, pp. 373-380, Aug. 1979
- <sup>7</sup> J. A. Stuller and Nancy Hubing, "New perspective for maximum likelihood time-delay estimation", *IEEE Trans. on Signal Processing*, vol. SP-45, pp. 513-525, Mar. 1997.
- <sup>8</sup> W.R. Hahn and S.A. Tretter, "Optimum processing for delay-vector estimation in passive signal arrays," *IEEE Trans. Inform. Theory* vol. IT-19, pp. 608-614, Sep. 1973.
- <sup>9</sup> L.C. Ng and Y. Bar-Shalom, "Multisensor multitarget time delay vector estimation," *IEEE Trans. Acoust., Speech, Signal Processing*, vol. ASSP-34, pp. 669-677, Aug. 1986.
- <sup>10</sup> W.R. Hann, " Optimum signal processing for passive sonar range and bearing estimation," *J. Acoust. Soc. Amer.*, vol. 58, no. 1, pp. 201-207, 1975.
- <sup>11</sup> V. H. MacDonald and P. M. Schultheiss, "Optimum passive bearing estimation in spatially incoherent noise environment," *J. Acoust. Soc. Amer.*, vol. 46, pp. 37-43, 1969.
- <sup>12</sup> P.E. Stoica and Nehorai, "Performance study of conditional and unconditional direction-of-arrival estimation", *IEEE Trans. on Signal Processing*, vol. SP-38, pp. 1783-1795, Oct. 1990.
- <sup>13</sup> M.A. Doron, H. Messer and A.J. Weiss, "Maximum likelihood direction finding of wideband sources," *IEEE Trans. on Signal Processing*, vol. SP-41, pp. 411-414, Jan. 1993.

- <sup>14</sup> M.A. Doron, "*Direction Finding of Narrowband and Wideband Sources*," PhD thesis, Tel-Aviv university, 1992.
- <sup>15</sup> A. Gelb, "Applied Optimal Estimation" pp 103, the MIT PRESS.
- <sup>16</sup> R.O.Nielsen, "Azimuth and elevation angle estimation with a three-dimensional array," *IEEE Trans. on Signal Processing*, vol. SP-19, pp. 84-86, Jan. 1994.
- <sup>17</sup> NASA Conference Publication "Joint acoustic propagation experiment(JAPE-91) workshop.

## Figure Captions

**Figure 1:** Schematic representation of the model and the coordinate system used here.

**Figure 2:** (a).The 2-D array geometry consisting of 7 randomly located microphones, which was used in the first two numerical simulations. (b) The 3-D array geometry, which was used in the third numerical simulation and the experimental measurements. (c) The 2-D array consisting of 3 microphones which was used in the last numerical simulation.

**Figure 3:** Azimuth estimation errors of the simulated 2-D array, as a function of the SNR. The source is positioned at an azimuth of  $60^\circ$  and an elevation angle of  $30^\circ$ . The solid line is the CRLB. The dots depict the magnitude of the errors of the first 25 individual runs (out of the 500 used). The circles depict the standard deviation of the TDDF estimator

**Figure 4:** The errors of the TDDF algorithm for the azimuth (a) and elevation (b) as a function of the azimuth, for the 2-D array shown in Fig. 2(a). The SNR is -6 dB, the elevation angle is  $50^\circ$ . The solid line is the CRLB, the circles depict the standard deviation of the TDDF estimator

**Figure 5:** The errors of the TDDF algorithm for the azimuth (a) and elevation (b) as a function of the elevation angle, for the 3-D array shown in Fig.2(b). The SNR is -6 dB, the azimuth is  $20^{\circ}$ . The solid line is the CRLB. The circles depict the standard deviation of the TDDF estimator, and the analytic variance expressions (Eq.23) are depicted as '+'. .

**Figure 6:** Azimuth estimation errors of the 3 microphone 2-D array used in the last simulation, as a function of the SNR. The source is positioned at an azimuth of  $30^{\circ}$ . The standard deviation of the TDDF estimate are depicted by '\*' and the standard deviation of the Beamformer is plotted by 'o'. .

**Figure 7 :** Experimentally measured azimuth errors of the TDDF algorithm as a function of the azimuth using the 3-D array. The source was a speech signal played from a loud speaker 1.5m' away from the array. The circles 'o' denotes the results measured in an anechoic chamber, and the '\*' indicates the results measured in an ordinary room. .

Figure 2

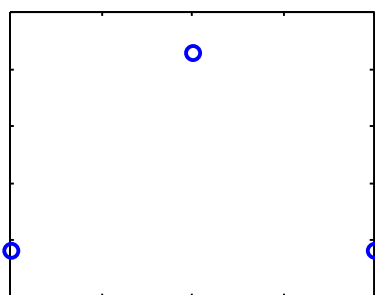
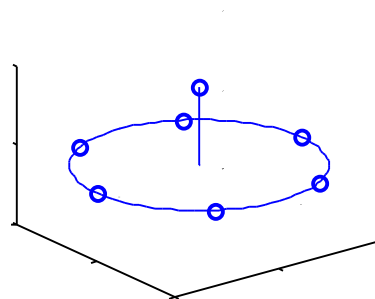
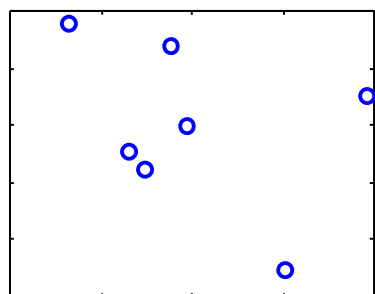


Figure 3

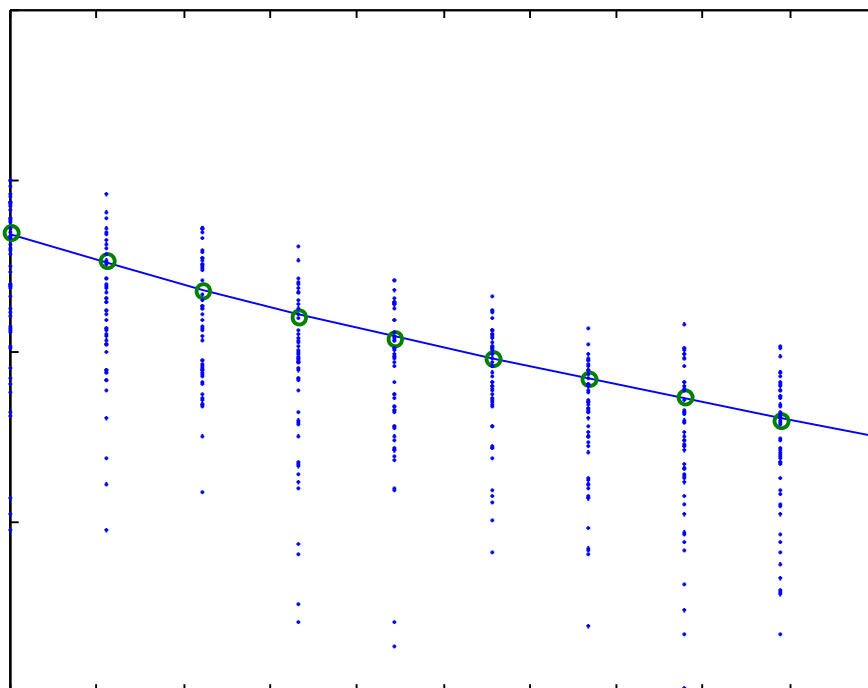


Figure 4

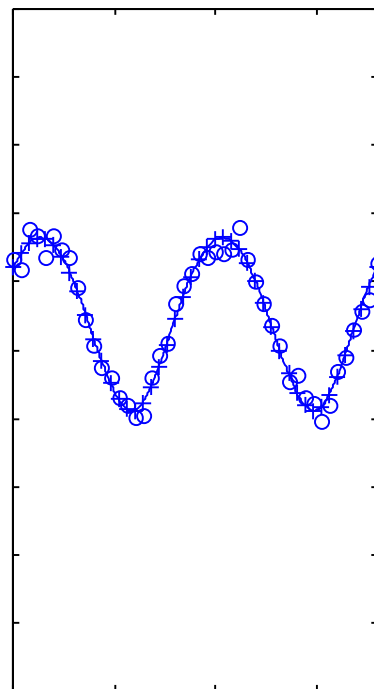
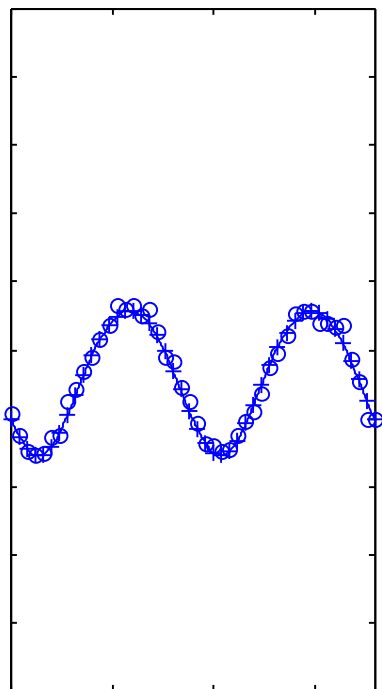


Figure 5

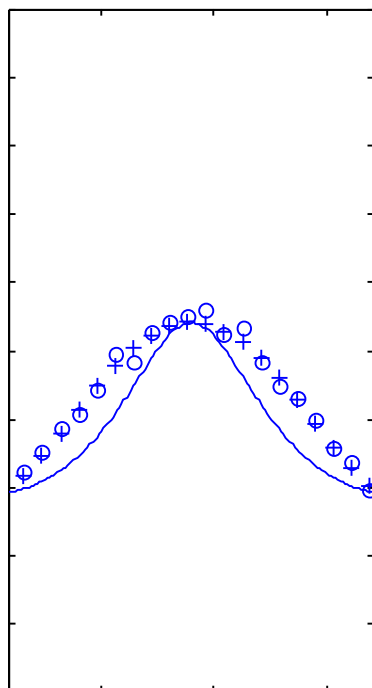
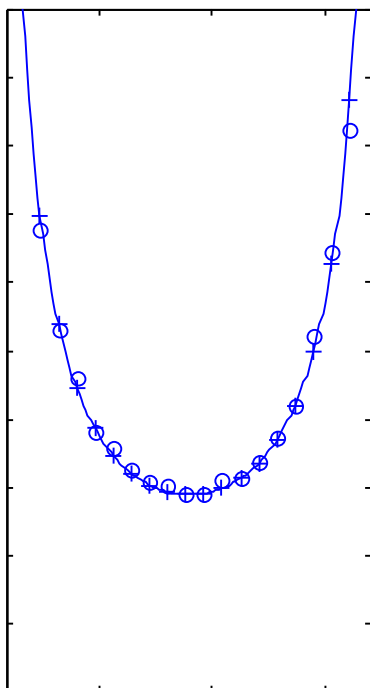


Figure 6

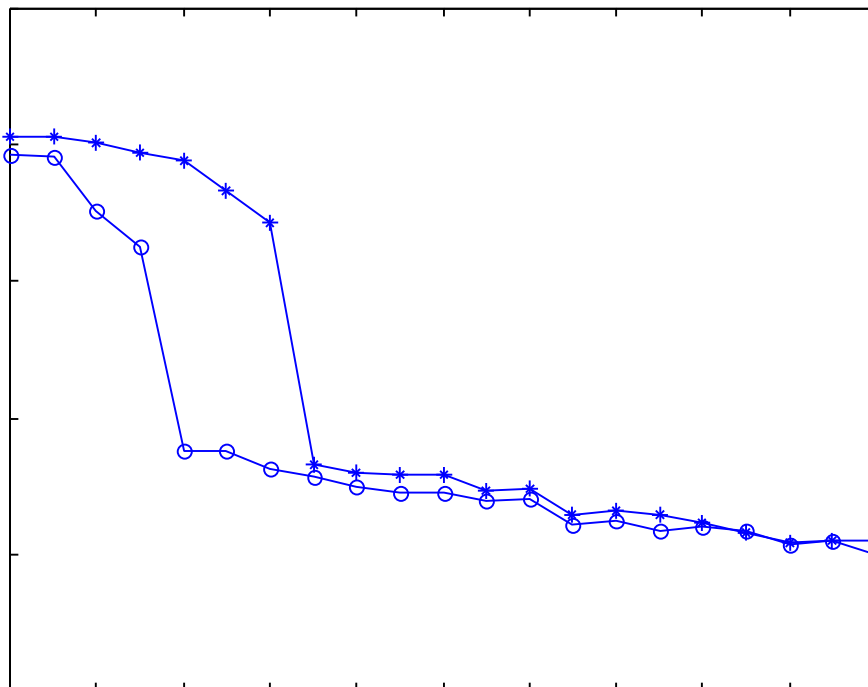


Figure 7

